ELSEVIER

Thermochimica Acta 374 (2001) 159–169

thermochimica acta

www.elsevier.com/locate/tca

Kinetics of Alder-ene reaction of Tris(2-allylphenoxy)triphenoxycyclotriphosphazene and bismaleimides — a DSC study

M. Sunitha, C.P. Reghunadhan Nair*, K. Krishnan, K.N. Ninan

Propellant and Special Chemicals Group, Vikram Sarabhai Space Centre, Trivandrum-695022, India

Received 27 September 2000; received in revised form 12 March 2001; accepted 12 March 2001

Abstract

Tris(2-allylphenoxy)triphenoxycyclotriphosphazene was reacted with three bismaleimides (BMI), viz. bis(4-maleimido phenyl)methane (BMM), bis(4-maleimido phenyl)ether (BME) and bis(4-maleimido phenyl)sulphone (BMS) via the Alder-ene reaction. The differential scanning calorimetric analysis of the blend manifested two distinct exotherms. The low temperature exothermic reaction was attributed to the Wagner-Jauregg reaction following the ene reaction and the strong exotherms at around 250–270°C to the cross-linking Diels–Alder reactions of the initially formed adducts. The Kinetic parameters, viz. activation energy (E) and pre-exponential factor (A) of the reactions were evaluated by Kissinger and Ozawa methods using the variable heating rate method. The kinetic data revealed that the Wagner-Jauregg reaction was disfavoured by electron-withdrawing nature of the BMI. The Diels–Alder reaction was facilitated by the electron-withdrawing nature of the bismaleimide. The activation energy for the first exothermic stage decreased and for the second major step increased on enhancing the stoichiometry of BMI in the blend for a given pair. The activation parameters served to predict the isothermal cure profiles of the blends and deduce the possible network structure under the given conditions of cure temperature and stoichiometry.

Keywords: Cyclotriphosphazene; Bismaleimides; Alder-ene reaction; Thermal polymerisation; DSC kinetics

1. Introduction

Despite the good attributes of processability and thermo-mechanical profile, the dominance of BMI systems in high performance composites for aerospace industry has been partially hampered by the inherent brittleness of the system [1–4]. A recent development in the toughening of BMI compositions is based on the reactive blends with allyl phenyl compounds, particularly diallyl bisphenols [5–7]. Commercial addition-cure formulations, based on co-reaction of bisallyl phenols and bismaleimides are the leading ones among tough matrices of carbon composite for advanced aerospace applications [8–10]. Maleimide reacts with allyl phenols through the Alder-ene reaction via an intermediate Wagner-Jauregg reaction [10,12]. The reaction mechanism and product profiles have been identified by studies on model compounds [12]. Alder-ene reactions of allyl phenyl derivatives such as Tris(2-allylphenoxy)triazine with BMIs have been used to derive thermosetting formulations [13]. With a view to develop thermally stable formulations based on cyclotriphosphazenes, we used the Alder-ene cure chemistry for designing the novel thermosets [14].

* Corresponding author. Tel.: +91-471-415-236/56; fax: +91-47-564-777/5.
E-mail address: cprnair@eth.net (C.P. Reghunadhan Nair).

0040-6031/01/$ – see front matter
PII: S0040-6031(01)00502-0

The protocol was to design allyl phenoxy substituted cyclotriphosphazenes and effect their cure using BMIs. Phosphazene moiety is known to confer thermal and flame retardancy to polymer systems [15–17].

The kinetics of Alder-ene reaction has not been reported. In this work, we report the kinetic analyses of Alder-ene reaction between Tris(2-allylphenoxy)-triphenoxycyclotriphosphazene and various BMIs using DSC technique. Differential scanning calorimetry (DSC) has been extensively used to determine the enthalpy and kinetics of the exothermic reactions of thermosetting polymers [27,28]. The Arrhenius activation parameters of different steps of reaction and their dependency on reactant stoichiometry and structure of BMIs have been examined.

2. Experimental

2.1. Materials

Bis(4-maleimido phenyl)methane (BMM), bis(4-maleimido phenyl)ether (BME), bis(4-maleimido phenyl)sulphone (BMS) were synthesised by standard procedure as described elsewhere [25]. Tris(2-allyl phenoxy)triphenoxycyclotriphosphazene (APCP) was synthesised from hexachlorocyclotriphosphazene (HCP) and phenol and 2-allyl phenol by a method being published [14]. APCP is a mixture of bis-, Tris- and tetrakis-allyl phenoxy substituted compounds in a proportion corresponding to an over all composition of Tris(allyl phenoxy) derivative, as confirmed from ^{31}P-NMR, ^{1}H-NMR and elemental analyses. The proportion of Tris compound is approximately 63% (computed from ^{31}P-NMR). Acetone was distilled from dry potassium carbonate.

2.1.1. Blending

APCP and the BMI of stoichiometric ratios 1:1, 1:1.5 and 1:2 were weighed and dissolved in acetone. The solvent was evaporated in vacuum and the resulting mixture was dried in vacuum at 50°C for 8 h.

2.2. Instrumental

2.2.1. DSC

DSC experiments were performed at varying heating rates in static air using a Mettler TA 3000 Thermal Analyser system in conjunction with a TC-10ATA processor and a standard DSC-20 apparatus. About 5 mg of the dry sample blend was weighed and encapsulated in 40 μl Al cups with a pierced lid and was used for DSC analysis. The temperature and heat flow calibrations were done by the recommended procedure using pure indium metal of melting point 156.6°C and heat of fusion, $\Delta H_f = 28.45$J/g. The peak temperature of all the samples were determined from the DSC curves by area integration of the exotherm and finding the point at which $\partial H/\partial T$ is null, with the help of dedicated software. When the peaks were not well resolved, experiments were repeated with varied quantities of the resin till defined maxima were obtained. In case the peak was ill defined or partly merged with another one, manual deconvolution was done to define the peak, and peak maximum was measured manually from the temperature–heat flow curve. This was associated with some error, reflected as proportionate standard deviations in the derived parameters.

3. Results and discussion

3.1. Synthesis of APCP

APCP was synthesized from HCP by reacting it with three equivalents of sodium phenolate followed by excess of sodium (2-allyl phenolate). The intermediate triphenoxy trichlorocyclotriphosphazene was analyzed for product distribution by GPC and ^{31}P-NMR. High resolution by GPC showed APCP to be essentially a mixture of three components. ^{31}P-NMR confirmed this observation. The NMR spectrum shown in Fig. 1 indicates that the product is a mixture of di(phenoxy)tetrachlorocyclotriphosphazene, symmetrical tri(phenoxy)-tri(chloro)cyclotriphosphazene, assymmetrical tri(phenoxy)-tri(chloro)cyclotriphosphazene, tetra(phenoxy)-di(chloro)cyclotriphosphazene and penta(phenoxy)monochlorocyclotriphosphazene. The assignment of the spectrum and relative mole fraction of all components are given in Table 1. The overall degree of substitution of the intermediate was estimated to be 2.85, on neglecting the extremely small concentrations of higher substitution compounds accounting for the remaining fractional substitution of 0.15. On substituting the remaining chlorine atoms of this intermediate with

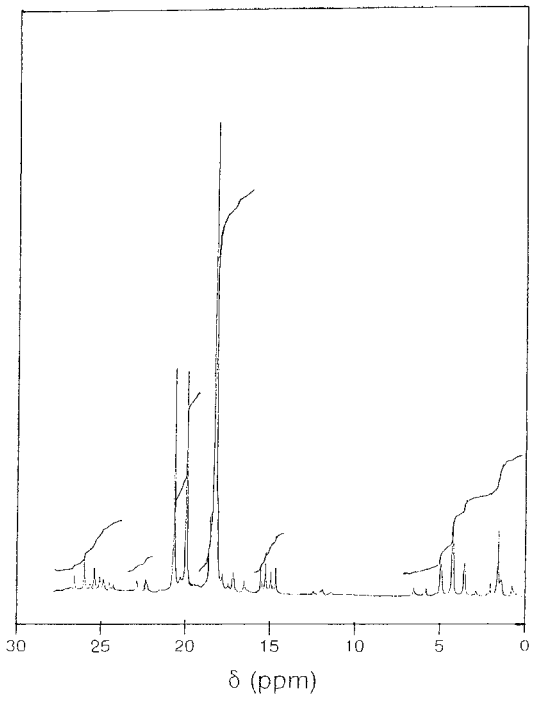

Fig. 1. ^{31}P-NMR spectrum of the intermediate — tri(chloro)-tri(phenoxy)cyclotriphosphazene.

sodium (2-allylphenolate), a mixture of products as detailed in Table 1 was obtained. The final product contains on the average three phenoxy groups and three allylphenoxy groups (as per NMR). The relative ratio of phenol and allylphenol was ascertained from the proton NMR of the final product. The NMR assignments are given below.

Proton NMR of APCP ($CDCl_3$); δ (ppm): 6.75–7.25 (m, 9H, aromatic), 5.75–6.1 (m, 1H, =CH allyl), 4.75–5.25 (m, 2H, $=CH_2$) and at 3.3–3.4 (d, 2H, $-CH_2$).

Thus, based on the product distribution of the intermediate which has been completely substituted to derive the end product, APCP consists of essentially four components as detailed in Table 1. The overall composition corresponds to three phenoxy and three allylphenoxy groups substituted on HCP. The ideal structure of APCP is depicted in Scheme 1.

3.2. DSC analyses

The non-isothermal DSCs of representative blends of APCP with three bismaleimides are shown in Fig. 2. On heating, the BMI and the blends undergo melting (Fig. 2). In cases of BMM and BME dual melting peaks were observed. The melting ranges are from 130 to 190°C depending on the nature of the blend and heating rate employed and increasing in the order BMM > BME > BMS. The melting is followed by two exotherms, which are overlapping in nature. Allyl phenyl derivatives are known to react with BMI by a sequence of reactions comprising of ene, Wagner-Jauregg and Diels–Alder reactions, collectively known as Alder-ene reaction [10,12]. The accepted reaction sequences for an ideal blend are shown in Scheme 2. Previous DSC analyses of similar reactive blends have revealed the existence of two or three distinct exotherms in league with the Alder-ene reaction sequences [18,19]. Accordingly, the ene reaction occurs at 100–190°C. Since this coincides with the melting endotherm, corresponding exotherms could barely be differentiated to facilitate a comparison and

Table 1
Characteristics of the components of APCP

Component in intermediate	^{31}P chemical shifts, signal nature, integration[a]			Mole fraction	Contribution towards functionality of intermediate	Product after substitution by allylphenol
	PCl_2	P(OPh)Cl	$P(OPh)_2$			
Diphenoxy	4.38 (t)	19.27 (d)	–	28.32	0.58	Tetrakis allyl
Symmetrical triphenoxy	–	17.14 (d)	–	5.01	1.51	Symmetrical Trisallyl
Asymmetrical triphenoxy	3.06 (dd)	14.7 (dd)	23.92 (dd)	15.43	0.46	Asymmetrical Trisallyl
Tetraphenoxy	–	21.75 (d)	24.44 (t)	2.81	0.12	Bisallyl
Pentaphenoxy	–	19.2 (t)	25.3 (d)	33.4	0.17	Monoallyl

[a] (s) Singlet; (d) doublet; (t) triplet; (dd) doublet of a doublet.

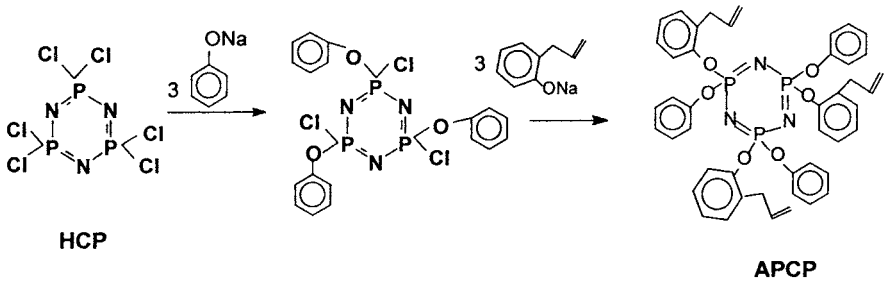

Scheme 1. Synthesis of APCP.

kinetic calculation. The first exotherm (190–215°C) in the present case can therefore be attributed to the Wagner-Jauregg step and the second to the extended Diels–Alder reaction and polymerisation of the unreacted monomers if any.

Although APCP is a mixture of cyclotriphosphazene of varying degree of substitution of the functional group (i.e. allyl phenoxy), the component molecules have practically the same size and molar masses. The difference in substitution pattern is not expected to lead to any significant variation in the reactivity of the allyl phenoxy groups located on different phosphazene rings. Throughout the work, the same composition was used to study kinetics of reactions of blends with different BMIs to avoid errors arising out of variation in distribution of the components of the mixture.

APCP was blended with three BMIs, viz. BMM, BME and BMS in the ratio 1:2.0. In the case of BMM, three different stoichiometric compositions,

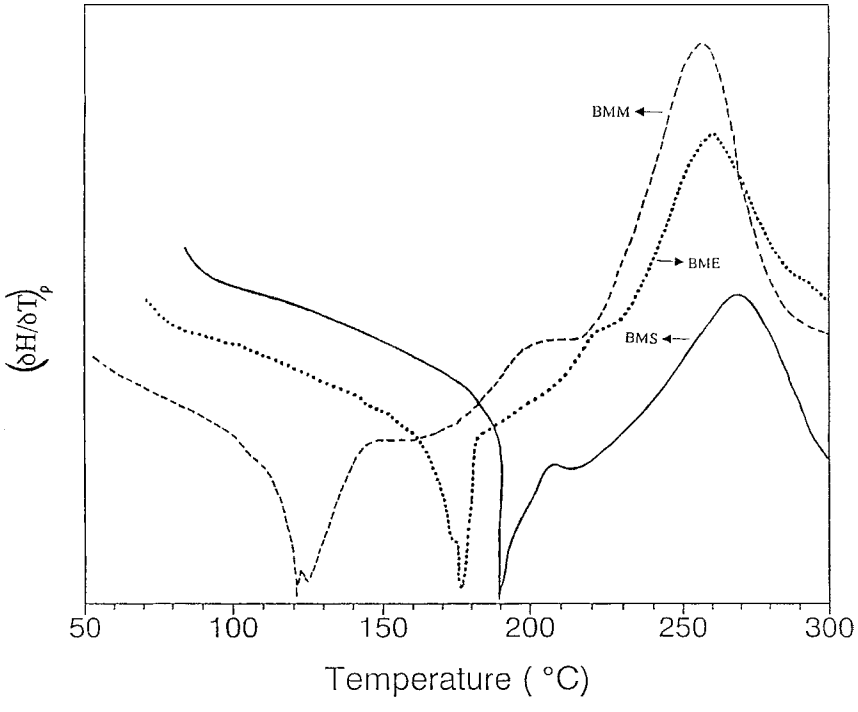

Fig. 2. DSC curves of BMI/APCP systems: (- - -) BMM (1:1.5); (· · ·) BME (1:2); (—) BMS (1:2). Heating rates: 7°C/min for BMM and BME; 10°C/min for BMS.

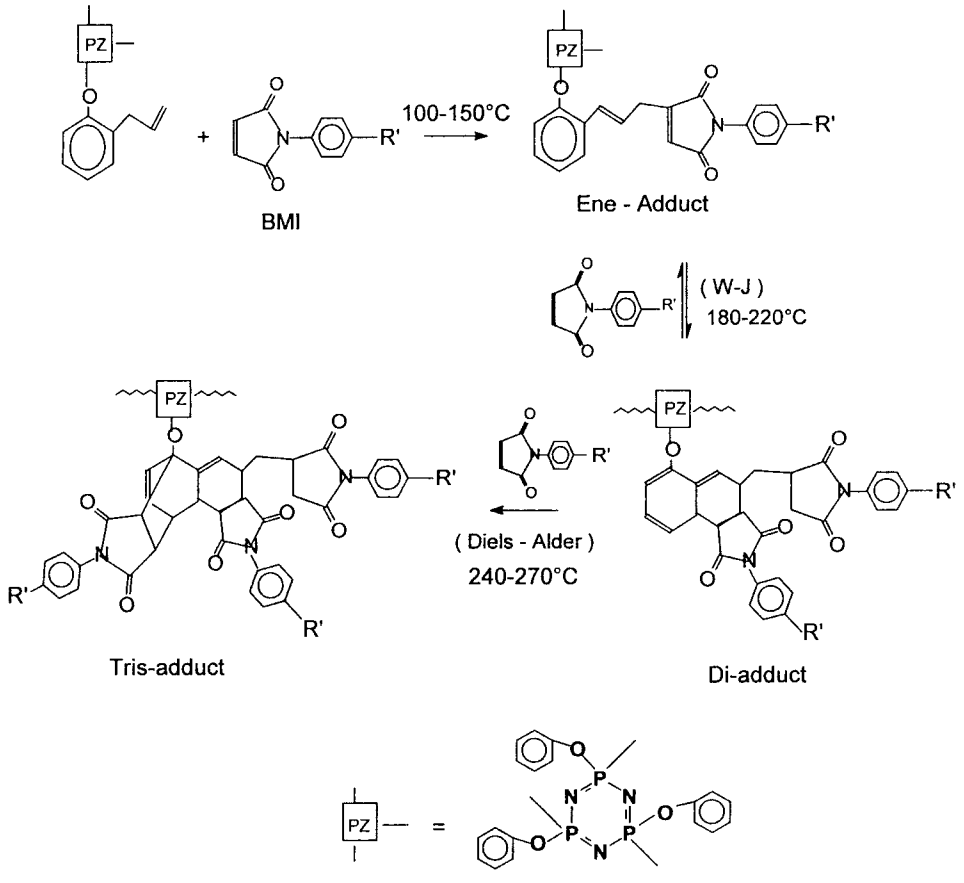

Scheme 2. Sequences of Alder-ene reaction.

viz. 1.1, 1:1.5, 1:2.0 were used. The DSC data are compiled in Table 2. The T_{m1} and T_{m2} represent the peak maximum temperatures for Wagner-Jauregg and Diels–Alder reactions, respectively. The T_m values for the W-J reaction were lower for BMM in comparison to BME. All the three systems exhibited nearly identical temperature profile for the second major step, although BMM exhibited slightly higher temperature in comparison to the other two. Increasing BMI stoichiometry marginally shifted the cure maximum to higher temperature regime, in the case of BMM.

Table 2
DSC peak maximum temperatures at different heating rates for polymer blends

Heating rate, Φ (°C/min)	BMM (1:1)		BMM (1:1.5)		BMM (1:2)		BME (1:2)		BMS (1:2)	
	T_{m1}	T_{m2}	T_{m1}	T_{m2}	T_{m1}	T_{m2}	T_{m1}	T_{m2}	T_{m1}	T_{m2}
2	–	–	179	221	170	242	190	225	190	208
5	195	243	189	242	197	255	200	250	198	245
7	204	249	205	251	200	263	212	256	200	259
10	205	257	211	257	223	272	217	265	206	266
15	220	267	220	270	224	280	230	276	210	277

3.3. Kinetic analysis

The kinetic analyses of the two steps were done by the variable heating rate method based on the methods of Kissinger [20] and Ozawa [21–23]. Recently, a similar approach was used to study the kinetics of Claisen rearrangement of diallyloxy bisphenols [24].

The peak maxima (T_m) for two stages of reactions and for various stoichiometric combinations obtained from DSC analysis are given in Table 2. The values showed a regular increase with increase in heating rate. The non-isothermal integral methods were not employed for the kinetic analyses because the exothermic reactions, particularly the low temperature ones, are not resolved and hence not amenable for area integration. Instead, the two well-known methods, viz. Kissinger and Ozawa methods based on variable heating rate which depend on peak maxima in DSC were employed for the purpose, where the apparent variations in activation energy caused by heating rates are also taken care of. Moreover, these methods do not invoke reaction order n or fractional conversion a in deriving the kinetic parameters. The final forms of Kissinger [20] and Ozawa [21–23] equations, used for finding the activation parameters are given below.

Kissinger equation:

$$\frac{2.303\,\mathrm{d}[\log(\phi/T_m^2)]}{\mathrm{d}(1/T_m)} = -\frac{E}{R} \tag{1}$$

where T_m is the temperature corresponding to the maximum in the DSC exotherm at a heating rate ϕ.

From the slope of the linear plot of $\log(\phi/T_m^2)$ against $1/T_m$, E can be calculated.

Ozawa equation:

$$\frac{2.15\,\mathrm{d}[\log(\phi)]}{\mathrm{d}(1/T_m)} = -\frac{E}{R} \tag{2}$$

where E was obtained from the slope of the plot of log ϕ against $1/T_m$.

The E-values obtained by Ozawa method needed refinement by iteration. This was done based on a two-term approximation for the Arrhenius temperature [29]

$$P(x) = \mathrm{e}^{-x}\left[\frac{(x+1)}{(x+3)}\right], \text{ where } x = \frac{E}{RT} \tag{3}$$

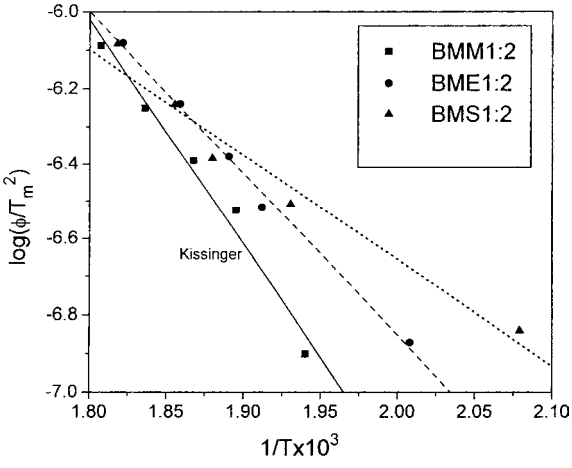

Fig. 3. Kinetic plots by Kissinger method.

The theoretical slope (D) of the above equation is $-1-2/x+1/(1+x)-1/(x+3)$. The process of iteration was continued to get a constant value for $E = 2.303 \times \text{slope}(\exp)/D$. This refinement is recommended for Ozawa method in ASTM E 698 [30]. Typical kinetic plots by Kissinger and Ozawa methods are shown in Figs. 3 and 4, respectively.

A was found in both cases from the relation

$$A = \frac{\phi E\,\mathrm{e}^{E/RT_m}}{RT_m^2} \tag{4}$$

The computed activation parameters are given in Table 3 for all the blend compositions and for two

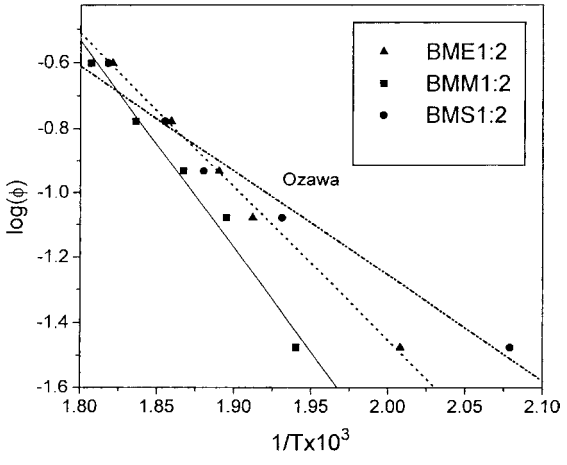

Fig. 4. Kinetic plots by Ozawa method.

Table 3
Kinetic parameters for different reactions

System	Reaction step	Kissinger		Ozawa		E (kJ/mol) for homopolymerisation [25]
		E (kJ/mol)	A (s^{-1})	E (kJ/mol)	A (s^{-1})	
BMM (1:2)	I	54.6 ± 7.1	3.62×10^3	54.9 ± 7.1	4.02×10^3	76.9
	II	113.5 ± 8.9	6.47×10^8	113.7 ± 8.9	6.88×10^8	
BMM (1:1.5)	I	75.3 ± 10.4	7.81×10^5	75.5 ± 10.4	6.42×10^5	
	II	84.3 ± 2.5	1.09×10^6	84.7 ± 2.5	1.21×10^6	
BMM (1:1)	I	75.9 ± 17.0	1.31×10^6	76.3 ± 17.0	1.52×10^6	
	II	96.3 ± 4.5	2.15×10^7	94.3 ± 4.4	1.88×10^7	
BME (1:2)	I	85.9 ± 11.3	9.15×10^6	86.2 ± 11.3	9.81×10^6	119.6
	II	81.7 ± 3.4	4.83×10^5	82.0 ± 3.4	5.14×10^5	
BMS (1:2)	I	175.7 ± 13.2	2.78×10^{17}	175.85 ± 6.1	2.9×10^{17}	
	II	53.3 ± 13.2	4.51×10^2	53.5 ± 6.2	4.75×10^2	

reaction steps. Both the methods give nearly identical values for a given reaction.

3.4. Reaction mechanism

A close examination of the DSC results and kinetic data showed that the Wagner-Jauregg reaction, essentially involving the Diels–Alder addition of BMI to the ene adduct showed a strong dependency on the electron density of the BMI. The electron-deficient BMS was found to have significantly higher activation for this reaction. However, it can be concluded that this step which is known to be reversible [13], is facilitated by electron density of the π-bond of BMI. On the other hand, the second major polymerisation step involving the Diels–Alder addition of BMI to the initially formed Wagner-Jauregg adduct was facilitated by the electrophilicity of the dienophile. Thus the trend in activation energy, BMS < BME < BMM is strictly in accordance with the decreasing electrophilicity of the double bond of BMI.

It is known that Diels–Alder reaction is facilitated by the increased electrophilicity of the dienophile. Since a reverse trend was observed for the Wagner-Jauregg reaction, it may be concluded that this reaction may be following a mechanism different from the conventional Diels–Alder reaction although the final product looks like a Diels–Alder adduct. The E-values for the second step are different from those reported for the thermal homopolymerisation of the BMIs, estimated by Rogers method [25], which are given in Table 3 for BMM and BME. This indicates that this exotherm is not due to the thermal homopolymerisations of BMIs, the probability for which is less, particularly when the BMI is stoichiometrically deficient in the blend.

Both reaction steps were identified for all the stoichiometry. This implies that all the sequences in the Alder-ene reactions could occur parallely when the system is heated dynamically, or at a stretch at high temperature. Thus, the network structure could depend upon the heating schedule and the stoichiometry. The reaction sequences in an ideal case of blend is shown in Scheme 2.

3.5. Effect of stoichiometry

The effect of stoichiometry of BMI + APCP on the phenomenological and kinetic aspects of the reaction was studied by preparing a typical blend of BMI + APCP in the ratio 1:1, 1:1.5 and 1:2.

It is reported that optimum stoichiometry for allylbismaleimide reaction is 1:3 [9–12]. However in most of the cases, a lower stoichiometry of the BMI is preferred in order to reduce the cross-link density of the network. In the present study also, the stoichiometry of BMI was kept to a maximum of 1:2. This could also avoid the possible contribution of the homopolymerisation of BMI at higher temperature and minimise the effect of its contribution in the present kinetic evaluation. The activation parameters for the two steps for three different stoichiometries were calculated and their values are also included in Table 3. The activation parameters are normally

expected to be independent of stoichiometry and the trend is followed up to a BMM stoichiometry of 1:1.5. However, the blend composition (1:2) showed large variation in E and A values of both the stages of reactions. When BMM stoichiometry is enhanced to 1:2, the Wagner-Jauregg reaction is found to be facilitated while the high temperature cure requires higher activation. This may also be due to probable changes in reaction mechanism at higher BMI-content. The enhanced activation energy for the Diels–Alder reaction may be attributed to the effect of diffusion control in the kinetics of this cross-linking step, as the concentration of the cross-linking agent (BMI) is increased in the blend.

The kinetic parameters derived form the present DSC study has been particularly used to compare the relative reactivities of different reaction steps of APCP with various BMIs under identical reaction conditions. In these perspectives, the derived kinetic parameters are useful and make sense. The kinetic parameters from DSC for solid state reactions may not make sense to define the absolute reactivity, etc. as normally inferred from normal reaction kinetics in closely defined systems. However, the derived kinetic parameters can be correlated to the reactivities particularly in temperature regimes, where the reactants retain their liquid consistency or are sufficiently mobile in order not to invoke the phenomena such as diffusion, etc. The kinetic parameters derived from the solid state reactions such as the later part of the Diels–Alder reaction, at best have only empirical significance and are useful for comparing reactivities and for predicting the isothermal cure profiles at a given temperature.

3.6. Prediction of Isothermal cure profile and network structure

The kinetic modeling is generally used for the cure time–temperature prediction of polymer systems.

The equation relating time, temperature and fractional conversion for any step is given as

$$\alpha = 1 - \{1 - A(1-n)t\,\mathrm{e}^{(-E/RT)}\}^{1/1-n} \qquad (5)$$

where α is the fractional conversion, A the pre-exponential factor, n the order of the reaction, t the time, E the apparent activation energy and T the temperature. Isothermal cure for the Diels–Alder reaction was calculated using the above equation for the three bismaleimides and for different stoichiometries for BMM + APCP. The reaction order, n was found from the Coats–Redfern treatment [26] for the second step using the relationship

$$\ln\left[\frac{g(\alpha)}{T^2}\right] = \ln\{(AR/\phi E)(1 - 2RT/E)\} - \frac{E}{RT} \qquad (6)$$

where

$$g(\alpha) = \left\{\frac{1-(1-\alpha)^{1-n}}{(1-n)}\right\} \text{ for } n \neq 1$$

and when

$$n = 1, g(\alpha) = -\ln(1-\alpha) \qquad (7)$$

where α was obtained by integration of the 2nd exotherm in typical cases, where the baseline is unambiguous. $\alpha = H_\alpha/H_t$, where H_α is the fractional enthalpy and H_t the functional enthalpy.

The plot of $\ln[(g(\alpha)/T^2)]$ for various assumed values of n ranging from 1–2.5, against reciprocal of absolute temperature (T) was performed. The correlation coefficient (r), for the linear fit for different values of n are given in Table 4.

In nearly all cases, the best value of n was found to be 2. Using this value of $n = 2$, α was calculated from the computed fractional enthalpy at each temperature T. The Coats–Redfern plot is shown for a typical case in Fig. 5.

Table 4
Determination of reaction order for the Diels–Alder reaction step for reaction of APCP/BMM (1:1.5), APCP/BME (1:2) and APCP/BMS (1:2) at a heating rate of 7°C/min by Coats–Redfern method

BMI system	Reaction order (n)	Correlation coefficient (r)
BMM	1	0.9410
	1.5	0.9720
	2	0.9810
	2.5	0.9760
BME	1	0.9607
	1.5	0.9800
	2	0.9799
	2.5	0.9674
BMS	1	0.9550
	1.5	0.9780
	2	0.9803
	2.5	0.9704

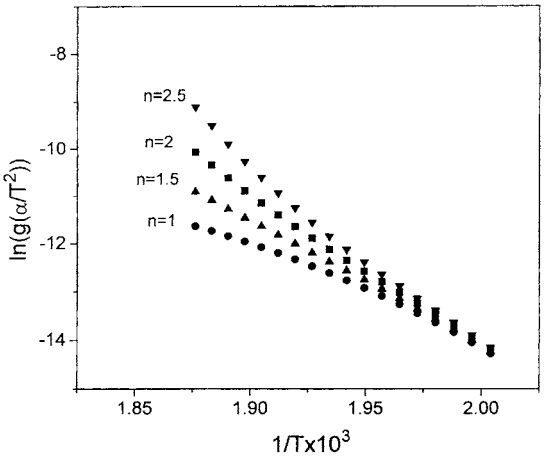

Fig. 5. Coats–Redfern kinetic plot for determination of reaction order for APCP/BMM for 1:1.5 blend.

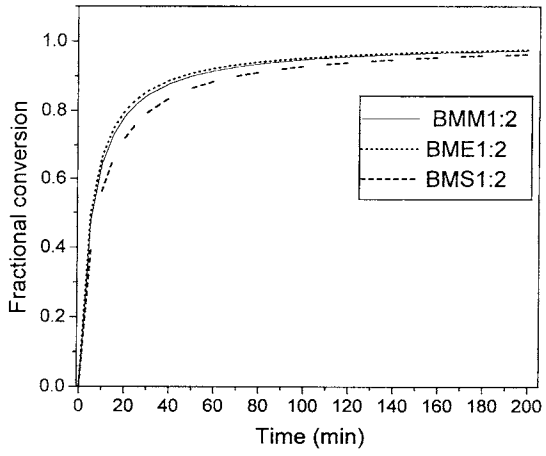

Fig. 6. Isothermal time-conversion data for the cross-linking reaction of the three reaction systems: BMM, BME, and BMS at 250°C.

Usually, Alder-ene adducts are cured by heating at 250°C. Heating is done stage-wise. The time-conversion data calculated for the final cross-linking reaction for the three reaction systems, viz. BMM, BME and BMS and for BMM at different stoichiometric ratios at 250°C are shown in Figs. 6 and 7, respectively. The cure is practically completed in about 2 h at 250°C. The difference among the various systems in cure behaviour is not significant. Comparison has been made for the final cure step only, since at this temperature the preceding ene and Wagner-Jauregg reaction will be occurring at a comparatively faster rate.

Since the cure reaction involves at least three major steps, the network structure could depend upon the cure temperature and on the stoichiometry. At a given temperature, all the three reactions are possible as evident from the DSC profile. The kinetics of each step is decided by its respective activation parameters and reactant concentration. For example, at low cure temperature and at low concentration of maleimide, the

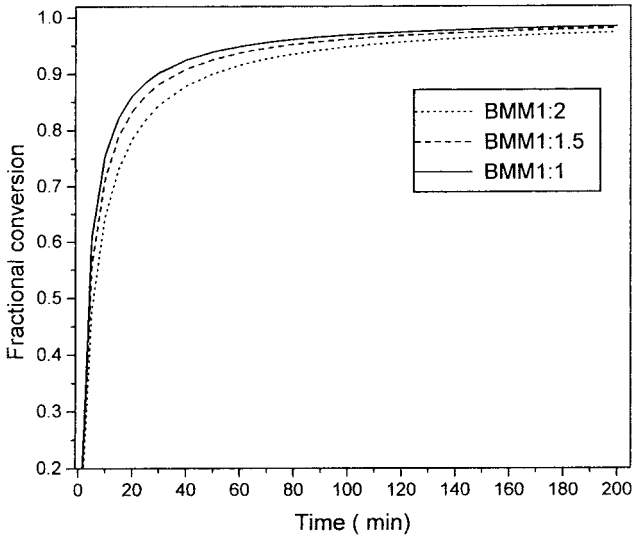

Fig. 7. Time-conversion profile for the cross-linking reaction of BMM at different stoichiometric ratios at 250°C.

cross-linked structure would be confined to the ene-adduct or to the Wagner-Jauregg adduct. At higher cure temperature, all the reactions are possible irrespective of stoichiometry. Calculation of the relative reaction rate (from the activation parameters) could lead to a first approximation of the network structure.

In majority of the cases, the cure is effected at 250°C. It can be assumed that the ene reaction precedes at a sufficiently faster rate at this temperature (in comparison to the Wagner-Jauregg and Diels–Alder reactions). For a 1:2 stoichiometry, one equivalent of the remaining bismaleimide can be considered to be distributed between the Wagner-Jauregg and Diels–Alder reactions. Since Diels–Alder reaction follows Wagner-Jauregg reaction, the relative conversions in the two cases can be calculated to the first approximation, by assuming that at any time given, the product of Wagner-Jauregg reaction from the reactant for Diels–Alder reaction. Assuming that the Wagner-Jauregg reaction is also second-order, the apparent relative conversion can be calculated using Eq. (5).

The conversion profile at three different cure temperatures for the typical case of BMM is shown in Fig. 8. It shows that at lower temperature, the Wagner-Jauregg reaction dominates over the Diels–Alder reaction and the network will be containing more of the structure resulting from the former. At higher cure temperature, the proportion of Diels–Alder structure increases in the network.

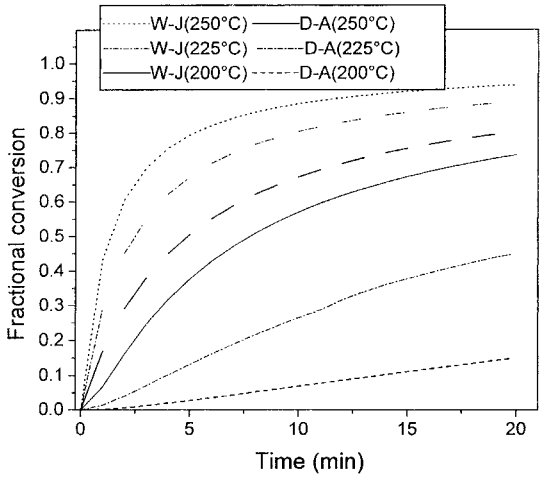

Fig. 8. Prediction of time-conversion profiles for the first and second step reactions at three different temperatures for BMM.

4. Conclusion

Tris(2-allylphenoxy)triphenoxycyclotriphosphazene was reacted with bis(4-maleimido phenyl)methane (BMM), bis(4-maleimido phenyl)ether (BME) and bis(4-maleimido phenyl)sulphone (BMS) via the Alder-ene reaction. The DSC of the blend manifested two major exotherms. The low enthalpy reaction at low temperature was attributed to the Wagner-Jauregg reaction following the ene addition and the strong exotherm at around 250–270°C was caused by Diels–Alder reactions of the initially formed adduct with BMI. The kinetics of the reaction, followed by non-isothermal DSC using the variable heating rate methods revealed that the Wagner-Jauregg reaction was disfavoured by electron withdrawing nature of the BMI. The major cross-linking reaction was facilitated by the electron deficiency of the BMI in league with the trend for Diels–Alder reaction. On increasing the BMI content beyond an allyl:BMI stoichiometry of 1:1.5, an apparent change in reaction mechanism was observed. The predicted isothermal cure profile shows that the reaction is faster in the case of BMM and is completed in 2 h at 250°C for all cases. Higher stoichiometry resulted in faster cure reaction. Prediction of isothermal reaction profile for the two steps shows that at lower cure temperature, the network is mostly composed of structures resulting from Wagner-Jauregg reaction. Diels–Alder structure dominates at higher cure temperature.

Acknowledgements

The authors thank their colleagues in the Analytical and Spectroscopy Division for the support in various analyses. The permission granted by VSSC to publish the results is gratefully acknowledged. M. Sunitha thanks Indian Space Research Organisation for grant of a fellowship.

References

[1] S.C. Lin, E.M. Pearce, High Performance Thermosets: Chemistry, Property and Applications, Hanser, Munich, 1994.

[2] R. Chandra, L. Rajabi, J. Macromol Sc., Rev Macrmol. Chem. Phys. C37 (1997) 61.

[3] P. Mison, B. Sillion, Progress in polyimide chemistry 1, Adv. Polym. Sci. 140 ((1998)) 137.
[4] H.D. Stenzenberger, P.M. Hergenrother, Addition polyimides, Adv. Polym. Sci. 117 (1994) 163.
[5] H.D. Stenzenberger, W. Romer, P.M. Hergenrother, B. Jensem, W. Breitigam, SAMPE J. 26 (1990) 75.
[6] G. Liang, A. Gu, Polymer Journal 29 (7) (1997) 553.
[7] L.A. Pilato, J. Michno, Advanced Composite Materials, Springer-Verlag, CH. 3 Heidelberg, 1994.
[8] C.P. Reghunadhan Nair, R.L. Bindu, K.N. Ninan, Recent developments, in: G. Radhakrishnan (Ed.), Phenolic Resins Metals, Materials and Processes, Meshap Publications, Mumbai 9 (2) (1997) 174.
[9] R.J. Morgan, A. Jurek, A. Yen, T. Donnelan, Polymer 34 (1993) 8355.
[10] R.J. Morgan, E. Shin, B. Rosenberg, A. Jurek, Polymer 38 (1997) 639.
[11] T. Wagner-Jauregg, Tetrahedron Lett. 13 (1967) 1175.
[12] D. Reyx, I. Campistron, C. Caillaud, M. Villatte, A. Cavedon, Makromol. Chem. Phys 196 (1995) 775.
[13] J.M. Barton, I. Hamerton, J.C. Jones, J.C. Stedman, Polymer 37 (1996) 4519.
[14] M. Sunitha, C.P.R. Nair, K.N. Ninan, J. Appl. Polym. Sci. (communicated).
[15] D. Kumar, G.M. Fohlen, J.A. Parker, J. Polym. Sci. 21 (1983) 3155.
[16] Y.W. Chen-Yang, H.F. Lee, C.Y. Yuan, J. Polym. Sci. P-A 38 (2000) 972.
[17] H.R. Allcock, Encyclopaedia of Polymeric Science and Engineering, Vol. 13, Wiley, New York, 1986, p. 31.
[18] C. Gouri, C.P.R. Nair, R. Ramaswamy, Polym. Int. (in press).
[19] R.L. Bindu, C.P.R. Nair, K.N. Ninan, J. Appl. Polym. Sci. (in press).
[20] H.E. Kissinger, J. Res. Nat. Bu. Stand. 57 (1956) 217.
[21] T. Ozawa, Therm. Anal 2 (1970) 301.
[22] T. Ozawa, Therm. Anal. 9 (1976) 369.
[23] T. Ozawa, Therm. Anal. 7 (1975) 601.
[24] C.P. R Nair, K. Krishnan, K.N. Ninan, Thermochim. Acta 1–7 (2000) 6270.
[25] K.N. Ninan, K. Krishan, J. Mathew, J. Appl. Polym. Sci. 32 (1986) 6033.
[26] A.W. Coats, J.P. Redfern, Nature 68 (1964) 201.
[27] M.A. Chitelli, R.B. Prime, E. Sacher, Polymer 12 (1971) 355.
[28] S.Y. Choi, SPEJ 26 (1970) 51.
[29] P.M. Madhusudhanan, K. Krishnan, K.N. Ninan, Thermochim. Acta 97 (1986) 217.
[30] ASTM E 698, Test methods for Arrhenius kinetic constants for thermally unstable materials.